



## OPEN Porcine milk small extracellular vesicles modulate peripheral blood mononuclear cell proteome in vitro

Gabriela Ávila<sup>1</sup>, Muriel Bonnet<sup>2</sup>, Didier Viala<sup>2,3</sup>, Sebastian Dejean<sup>4</sup>, Alessandro Agazzi<sup>1</sup>, Cristina Lecchi<sup>1</sup> & Fabrizio Ceciliani<sup>1</sup>✉

Small extracellular vesicles (EVs) are a subtype of nano-sized extracellular vesicles that mediate intercellular communication. EVs can be found in different body fluids, including milk. Monocytes internalize porcine milk EVs and modulate immune functions in vitro by decreasing their phagocytosis and chemotaxis while increasing their oxidative burst. This study aimed to assess the impact of porcine milk EVs on the porcine peripheral blood mononuclear cells (PBMC) proteome. Porcine PBMC were incubated with porcine milk EVs or medium as a control. Extracted proteins were then analyzed using nano-LC-MS/MS. A total of 1584 proteins were identified. The supervised multivariate statistical analysis, sparse variant partial least squares – discriminant analysis (sPLS-DA) for paired data identified discriminant proteins (DP) that contributed to a clear separation between the porcine milk EVs treated cells and control groups. A total of 384 DP from both components were selected. Gene Ontology (GO) enrichment analysis with ProteINSIDE provided the evidence that the DP with a higher abundance in porcine milk EVs, like TLR2, APOE, CD36, MFGE8, were mainly involved in innate immunity and the process of EVs uptake processes. These results provide a proteomics background to the immunomodulatory activity of porcine milk EVs and to the potential mechanisms used by immune cells to internalize them.

**Keywords** Milk small extracellular vesicles, Pig, PBMC, Immunomodulation, Phagocytosis, Proteomics

### Abbreviations

APOE	Apolipoprotein E
BP	Biological processes
BTN1A1	Butyrophilin subfamily 1 member A1
CSN1S1	Alpha-s1-casein
CSN1S2	Alpha-s2-casein
CSN2	β-Caseins
CSN3	κ-Casein
CTSH	Cathepsin H
eNOS	Endothelial nitric oxide synthase
EV	Extracellular vesicles
FDR	False discovery rate
GO	Gene ontology
DP	Discriminant protein
ERK1/2	Extracellular signal-regulated kinase
1/2FABP4	Fatty acid-binding protein 4
iNOS	Inducible nitric oxide synthase
LGALS3	Galectin-3
MFGE8	Lactadherin
Nano-LC-MS/MS	Nanoscale liquid chromatography coupled to tandem mass spectrometry
NK	Natural killer
NO	Nitric oxide

<sup>1</sup>Department of Veterinary and Animal Sciences, Università Degli Studi di Milano, Via dell'Università 6, 26900 Lodi, Italy. <sup>2</sup>INRAE, University of Clermont Auvergne, Vetagro Sup, UMRH, 63122 Saint-Genès-Champanelle, France. <sup>3</sup>INRAE, Metabolomic and Proteomic Exploration Facility, Proteomic Component, (PFEMcp), 63122 Saint-Genès-Champanelle, France. <sup>4</sup>Institute of Mathematics of Toulouse, University of Toulouse, CNRS, UPS, UMR 5219, 31062 Toulouse, France. ✉email: fabrizio.ceciliani@unimi.it

PBMC	Peripheral blood mononuclear cells
ROS	Reactive oxygen species
SASH3	SH3 domain-containing 3 protein
SLC34A2	Na(+)-dependent phosphate cotransporter 2B protein
sPLS-DA	Partial least square discriminant analysis
TLR	Toll-like receptor

Small extracellular vesicles (EVs) are nano-sized extracellular vesicles (30–160 nm) with an endosome-derived limiting membrane mediating intercellular communication in physiological and pathological conditions<sup>1,2</sup>. They can be produced and released by all cell types through exocytosis<sup>3</sup>. EVs carry a wide range of regulatory molecules (cargo) such as proteins, lipids, DNA, RNA (mRNA, and non-coding RNA, like miRNA), and metabolites<sup>1</sup>. These nanovesicles mediate near long-distance intercellular communication by targeting and transferring their cargo into recipient cells, altering their function<sup>4,5</sup>.

Over the last two decades, EVs have been demonstrated to induce, amplify, and suppress innate and adaptive immune responses. Indeed, EVs have been shown to modulate natural killer (NK) cell activation, macrophage and T cell differentiation, and monocyte chemotaxis<sup>6–8</sup>. Anti-inflammatory roles of EVs in human peripheral blood mononuclear cells (PBMC) and T cells have also been reported<sup>9</sup>.

EVs can be found in different body fluids, including milk<sup>10</sup>. Milk EVs are also thought to exert potential immunomodulatory effects, as human and bovine milk EVs containing functional RNA are taken up by human macrophages<sup>11,12</sup>. After suckling or oral administration, bovine, porcine, or murine milk EVs and their cargo can accumulate in piglets and mice peripheral tissues, like the liver, spleen, lung, and small intestine, that are rich in immune cells<sup>13</sup>, suggesting potential immunomodulation. Moreover, our previous *in vitro* study demonstrated that porcine milk EVs exert immunomodulatory effects on porcine monocytes by decreasing their phagocytosis and chemotaxis and increasing their reactive oxygen species (ROS) production<sup>14</sup>. However, the molecular mechanisms underlying the immunomodulatory activity of porcine milk EVs on porcine mononuclear cells are still unknown.

OMIC technologies, specifically proteomics – the large-scale study of the protein profile in a sample – provide a great option to unravel the molecular impact of porcine milk EVs on porcine PBMC immune response<sup>15</sup>. In previous studies, porcine PBMC proteome has been investigated, mainly in the context of infectious diseases<sup>16</sup>, stress<sup>17</sup>, pregnancy<sup>18</sup>, and characterization of the cell's protein profile<sup>19</sup>. Still, there is no information on the *in vitro* impact of milk EVs on porcine PBMC proteome. Therefore, this study covers this gap by describing for the first time the immunomodulatory capacity of porcine milk EVs on porcine PBMC proteome *in vitro*, using an untargeted proteomics approach.

## Results

### The proteome of porcine PBMC and identification of the molecular signature of porcine milk EVs treatment

A total of 1584 proteins, with at least two unique peptides, were identified and quantified in porcine PBMC (Supplementary Table S1). A multivariate sPLS-DA analysis was applied to determine the molecular signature of the porcine milk EVs treatment. The sPLS-DA model selected a total of 384 DP (approximately 25% of the total proteins identified) from both components (Supplementary Table S2), providing a good clustering between the two treatment groups (Fig. 1).

From the 384 DP, only the proteins from the sPLS-DA component 1 that strongly correlated together for each treatment group were selected to perform separate GO BP enrichment analyses. Of these proteins, 54 had the highest abundance in the milk EVs group, while 142 were in the control group (Supplementary Table S3).

### GO enrichment analyses of total DP identified by s-PLS-DA.

A GO enrichment analysis was performed to identify the global function of all 384 DP. These DP were annotated by 301 enriched (FDR < 0.05) GO terms within the BP category. The main enriched BP were related to cellular supramolecular fiber organization (GO:0097435), metabolic process (GO:0008152), actin cytoskeleton organization (GO:0030036), intracellular transport (GO:0046907), positive regulation of organelle organization (GO:0010638), translation (GO:0006412), regulation of vesicle-mediated transport (GO:0060627), gene expression (GO:0010467), immune system process (GO:0002376) and regulation of apoptotic signaling pathway (GO:2001233) (Fig. 2).

Among the most annotated BP were: gene expression (142), metabolic processes (92), immune system process (70) and intracellular transport (50) (Supplementary Table S4).

### GO and KEGG enrichment analyses and PPI of DP with the highest abundance in the milk EVs group

To further elucidate the specific role of the DP with the highest abundance in each group, separate GO enrichment analyses were performed. The 54 proteins with the highest abundance in the milk EVs group were annotated by 130 enriched (FDR < 0.05) GO terms within the BP category. These proteins were mainly involved in BP such as cellular detoxification (GO:1990748), response to diacyl bacterial lipopeptide (GO:0071726), nitric oxide-mediated signal transduction (GO:0007263), cGMP-mediated signaling (GO:0019934), positive regulation of tumor necrosis factor production (GO:0032760), positive regulation of endocytosis (GO:0045807), secretion (GO:0071706), immune system process (GO:0002376), ERK1 and ERK2 cascade (GO:0070371), regulation of body fluid levels (GO:0050878) and phagocytosis, recognition (GO:0006910). From these enriched BP, the ones with the highest number of annotated proteins were the immune system process with nine proteins, secretion with six proteins, and ERK1 and ERK2 cascade and regulation of body fluid with five proteins (Fig. 3A).

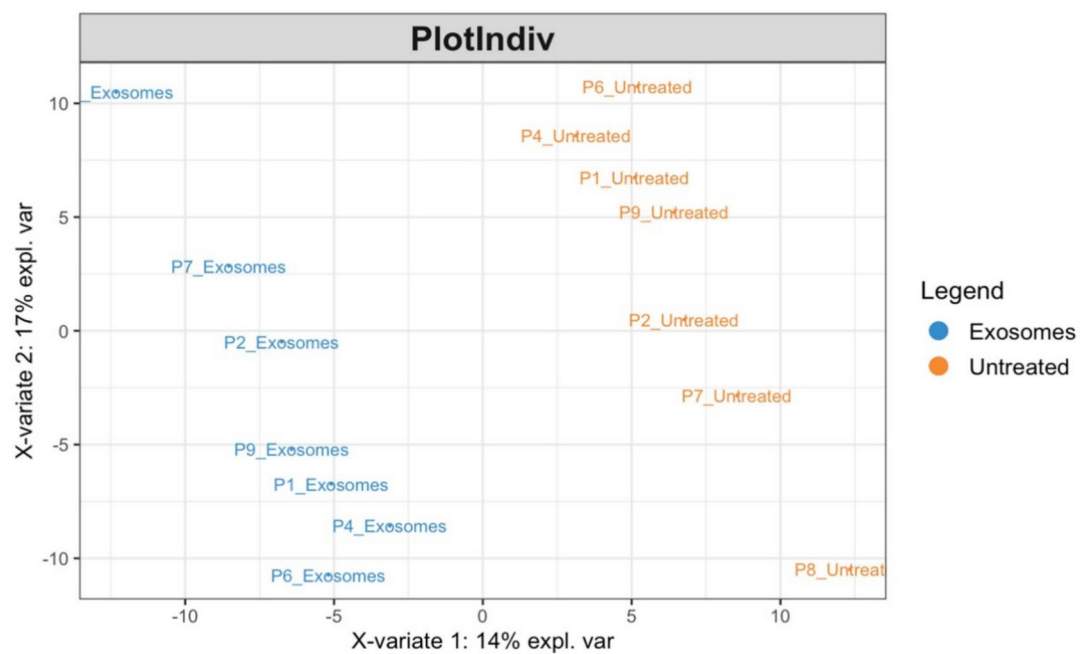


**Fig. 1.** Sparse partial least squares discriminant analysis (sPLS-DA) for paired data individual plot (PlotIndiv). The individual plot shows the similarities and relationship (clustering) between samples of the porcine milk EV (blue) and the untreated control (orange) treatment groups.

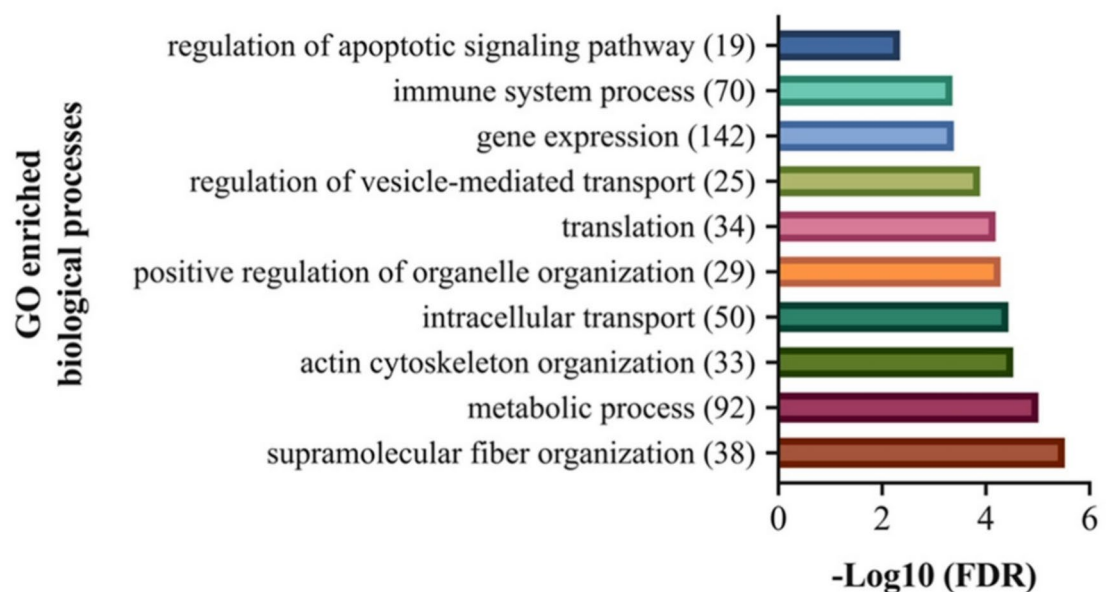


**Fig. 2.** Global enriched ( $P < 0.05$ ) Gene ontology (GO) terms within the biological process (BP) categories. The GO has annotated all 384 discriminant proteins (DP). GO terms enrichments are expressed as  $-\log_{10}$  (FDR) for visualization on graphs. The total number of proteins annotated by GO BP terms is shown in brackets.

CD36 and APOE were mainly annotated by almost all of these enriched BP. SASH3, CLU, and Cathepsin H (CTSH) were found in the immune system process, but CLU and CTSH were also found in positive regulation of endocytosis and ERK1 and ERK2 cascade, respectively. Moreover, TLR2 was found in the biological processes involved with the response to bacterial lipopeptide, immune system process, and secretion. In the latter and the regulation of body fluids, CSN2 and CSN3 were also found. Lastly, MFGE8 was only found in phagocytosis (Supplementary Table S5). The enriched GO CC and MF terms are shown in Supplementary Figs. S1 and S2, respectively. Additionally, only the phagosome (KEGG:04145) KEGG pathway was found to be enriched (Fig. 3B). Of the 54 DP proteins, 9 were involved in 4 PPI networks (Fig. 3C).

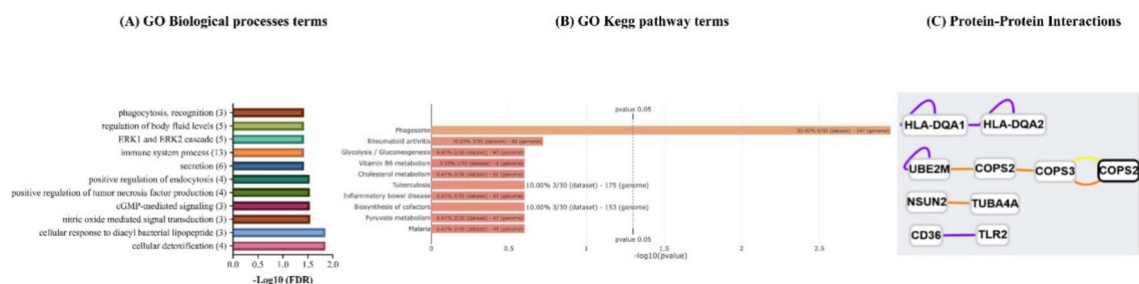


**Fig. 3.** Enriched ( $P < 0.05$ ) Gene ontology (GO) terms within: (A) the biological process (BP) category, and (B) KEGG pathways enrichment that have annotated the 54 discriminant proteins (DP) with the highest abundance in the porcine milk EVs group. GO terms enrichments are expressed as  $-\log_{10}(\text{FDR})$  for visualization on graphs. The total number of proteins annotated by GO BP terms is shown in brackets. (C) Protein-Protein Interaction (PPI) for the DP with higher abundance in the porcine milk EVs group.

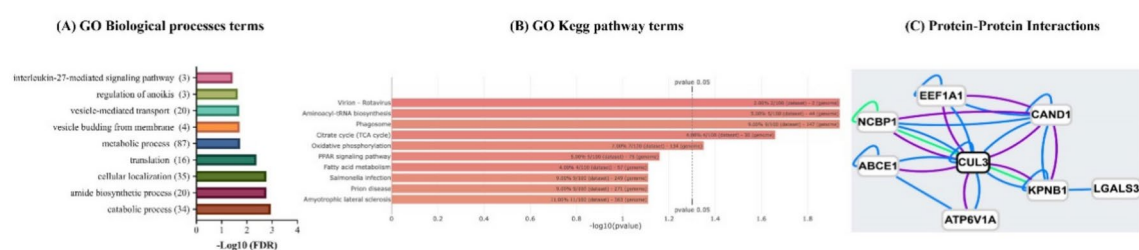


**Fig. 4.** Enriched ( $P < 0.05$ ) Gene ontology (GO) terms within: (A) the biological process (BP) category, and (B) KEGG pathways enrichment that have annotated the 142 discriminant proteins (DP) with the highest abundance in the control group (no milk EV). GO terms enrichments are expressed as  $-\log_{10}(\text{FDR})$  for visualization on graphs. The total number of proteins annotated by GO BP terms is shown in brackets. (C) Protein-Protein Interaction (PPI) for the DP with higher abundance in the control group.

### GO and KEGG enrichment analyses and PPI of DP with the highest abundance in the control group

A higher number of DP (142) was found to be more abundant in the control group. These proteins were annotated by 64 enriched ( $\text{FDR} < 0.05$ ) BP GO terms. These enriched GO terms were mainly related to the catabolic process (GO:0009056), amide biosynthetic process (GO:0043604), cellular organization (GO:0051641), translation (GO:0006412), metabolic process (GO:0008152), vesicle budding from the membrane (GO:0006900), vesicle-mediated transport (GO:0016192), regulation of anoxia (GO:2000209) and interleukin-27-mediated signaling pathway (GO:0070106) (Fig. 4A).

The enriched BP with the highest number of annotated proteins were: metabolic processes (87), cellular localization (35) and catabolic process (34) (Supplementary Table S6). The enriched GO CC and MF terms are shown in Supplementary Figs. S3 and S4, respectively. Additionally, the KEGG pathways: Virion-Rotavirus (KEGG:03271), Aminoacyl-tRNA biosynthesis (KEGG:00970), the phagosome (KEGG:04145), Citrate cycle (TCA cycle) (KEGG:00020) and Oxidative phosphorylation (KEGG:00190) were also found to be enriched (Fig. 4B). Of the 142 DP proteins, 8 were involved in 1 major network (Fig. 4C).

### Average log fold-change (logFC) of the abundances of the DP identified with sPLS-DA

Lastly, to identify and focus on key DP that presented greater changes in their abundance after porcine milk EVs treatment, the average logFC of the raw abundances of the proteins from the cells treated with milk EVs was calculated (Fig. 5).

The protein with the most significant change in the abundance ( $\log\text{FC} > 100$ ) between the milk EVs and control was CSN2. Other proteins with higher abundances in the milk EVs group were found, including BTN1A1, CSN1S1, CSN1S2, MFGE8, and SLC34A2 ( $\log\text{FC} > 5$ ). On the other hand, FABP4 ( $\log\text{FC} < 0.5$ ) and LGALS3 ( $\log\text{FC} < 1$ ) showed the lowest abundance in the milk EVs group.

### Discussion

The present study describes the proteome of porcine PBMC after stimulation with milk EVs, demonstrating that milk EVs co-incubation enriches biological processes (BP) involved in phagocytosis, endocytosis, and, more generally, inflammatory response, and immune reaction. These findings support, at the proteomics level, our recent findings that EVs have an immunomodulatory activity on porcine monocytes<sup>14</sup>.

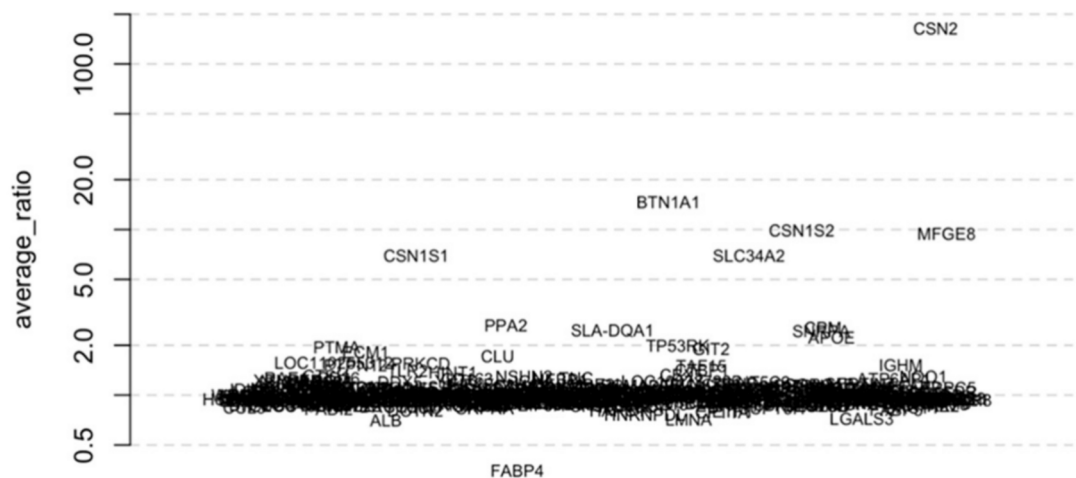


**Fig. 5.** Average log fold-change (logFC) of protein raw abundances of the 384 discriminant proteins (DP) selected by sPLS-DA. The y-axis shows the average logFC (ratio) of the raw abundances from all seven biological replicates (samples) after treatment of porcine milk EV. Proteins are represented with their corresponding Gene ID.

#### **Global biological processes enriched by the DP selected by sPLS-DA**

The sPLS-DA model selected the most discriminant proteins (DP), allowing an evident clustering of the samples between the EVs-treated PBMC and the control groups<sup>20</sup>. Consistently with the immunomodulatory activity on PBMC previously observed, the GO enrichment analysis revealed that EVs activate BP-like actin cytoskeleton organization and cellular supramolecular fiber organization, intracellular transport, positive organelle organization regulation, vesicle-mediated transport, all of them involved in chemotaxis-related processes and both BP associated with chemotaxis, phagocytosis, and cell communication<sup>21–25</sup>.

#### **Biological processes enriched by DP with the highest abundance in the EVs-treated PBMC toward changes in phagocytosis and inflammatory response**

Separate GO enrichment analyses were performed using the DP with the highest abundance in each group to elucidate further the differences between the two groups. The 54 DP with the highest abundance in the porcine milk EVs group enriched BP in the immune system process, including phagocytosis, positive regulation of tumor necrosis factor production response to diacyl bacterial lipopeptide, and nitric oxide-mediated signal transduction.

Phagocytosis plays an essential role in the uptake of EVs by monocytes and macrophages<sup>26,27</sup>. Several proteins involved in phagocytosis were found as highly abundant in the EVs -treated PBMC, namely glycoprotein IIIb (CD36), milk fat globule-EGF factor 8 (MFGE8 – lactadherin), extracellular signal-regulated kinase 1/2 (ERK1/2), and apolipoprotein E (APOE).

CD36 is one of the proteins involved in almost all enriched BP. CD36 is a PBMC membrane glycoprotein that participates in the identification and phagocytosis of apoptotic cells, ROS production, and macrophage modulation<sup>28–30</sup>. The fact that CD36 is related to phagocytosis and endocytosis, the main mechanisms of EV internalization, explains the uptake of porcine milk EVs by porcine monocytes, previously demonstrated by our team<sup>14</sup>.

The milk fat globule-EGF factor 8 (MFGE8 – lactadherin) is a phosphatidylserine-binding glycoprotein secreted and expressed by macrophages that promotes the engulfment of apoptotic cells and vesicles<sup>31,32</sup>. It is also one of the immune components found in milk, specifically in milk fat globules, and highly enriched in milk EVs<sup>33,34</sup>. MFGE8 may also play a role in the intestinal immune system of newborns<sup>35</sup> and is involved in EV phagocytosis by macrophages and monocytes<sup>36</sup>. The extracellular signal-regulated kinase 1/2 (ERK1/2) cascade signaling pathway regulates several stimulated cellular processes, including, among others, migration, apoptosis, and stress response<sup>37</sup>. A previous study showed that EVs activated the ERK1/2 cascade and that its activity is necessary for efficient EVs uptake via lipid raft-mediated endocytosis<sup>38</sup>. It was previously found that EVs and their miRNA cargo can modulate the ERK1/2 signaling pathway to induce immunomodulatory effects such as reducing macrophage migration<sup>39</sup>. Finally, APOE—a major protein component of very-low and high-density lipoproteins mainly expressed by monocytes/macrophages—has been shown to exert anti-inflammatory roles, including reducing the migration of some cells<sup>40,41</sup>. Our results are consistent with previous reports, demonstrating that EVs released by anti-inflammatory (M2) macrophages increase the levels of APOE in the cancer cells and modulate their migratory capacity through the transfer of functional APOE<sup>42</sup>. The presence of APOE in porcine colostrum and milk EVs has already been reported<sup>43</sup>. The function of APOE in modulating the migration of different cell types seems to be mediated in a MAPK/ERK1/2, explaining why this DP was also found annotated in the ERK1/2 cascade BP<sup>44</sup>.



Some significant DP are also involved in modulating inflammatory response, like TLR2. Our results agree with previous studies in different models. For example, EVs isolated from systemic lupus erythematosus patients enhanced the production of TNF- $\alpha$  and other proinflammatory cytokines via the TLR-related pathways<sup>45</sup>.

Another crucial immune response process is the production of nitric oxide (NO) and its mediated signaling transduction. Both NO-mediated signaling transduction and cGMP-mediated signaling were enriched after treatment with milk EVs. One is the inducible nitric oxide synthase (iNOS), which produces NO<sup>46</sup>. These results are consistent with previous studies on other cellular models, where EVs derived from hypoxic cardiomyocytes promoted NO production in endothelial cells<sup>47</sup>. Moreover, the release of EVs from senescent macrophages containing iNOS has been reported; bovine milk EVs containing miR-155-5p – an essential regulator of eNOS and NO – increased eNOS in endothelial cells. This suggests that EV cargo might also play an important role in modulating NO production<sup>48,49</sup>.

Further proteins such as Clusterin (CLU) and SAM and SH3 domain-containing 3 protein (SASH3) were annotated in several previously described immune-related processes. CLU, also known as apolipoprotein J, is a ubiquitously expressed glycoprotein and a known extracellular chaperone that has been shown to exert immunomodulatory and anti-inflammatory effects such as modulation of antimicrobial responses, facilitation of apoptotic cell clearance and suppression of kidney macrophage infiltration<sup>50,51</sup>. CLU can be found in both milk and milk EVs and is one of the proteins implied to modulate the immune response of the offspring<sup>52</sup>. SASH3 is an adaptor protein involved in signal transduction<sup>53</sup>. These results suggest that EVs can modulate different aspects of innate and adaptive immunity, confirming their pleiotropic functions.

In the secretion and regulation of body fluids BP, proteins such as  $\beta$ -caseins and  $\kappa$ -casein (CSN2 and CSN3) were found. Caseins are the most abundant proteins in milk, and, besides many other functions<sup>54</sup>, they enhance EV uptake, altering the gene expression in blood cells<sup>55</sup>. The purification procedure of EVs from milk, combining high speed centrifugation with size exclusion chromatography, should rule out as much as possible that casein from milk sticks over the membrane to purified EV. Still, we may not completely rule out this event, and therefore, we cannot exclude that the casein found in the PBMC proteome were part of the EV cargo.

Overall, these results provide a molecular background to previously reported *in vitro* activity of EV on porcine PBMC<sup>14</sup>. *In vitro* studies demonstrated that EVs induce changes in porcine monocyte chemotaxis, phagocytosis, and ROS production. These findings confirmed that BP involved in the same immune-related activities are enriched. Therefore, we can hypothesize that EVs can function as potential nanocarriers of immunomodulatory molecules that participate in immunity transmission from the mother to the offspring, helping modulate the newborn immune system.

### Biological processes enriched by DP with the highest abundance in the control group

In contrast to what was observed in the milk EVs group, the 142 DP with a higher abundance in the control group were annotated mainly by very general BP, such as different metabolic processes, cellular organization, translation, and vesicle-mediated transport.

Other processes related to cell death and immune-related processes, such as regulation of anoikis, a subtype of apoptosis caused when cells lose their adhesive capability<sup>56</sup>, and interleukin-27-mediated signaling pathway. Interleukin-27 (IL-27) is a cytokine produced by monocytes, macrophages, and DC, with both pro- and anti-inflammatory and other immunoregulatory functions, and is also involved in cell proliferation, differentiation, and expression of cytokines<sup>57</sup>.

Altogether, these results highlight that after porcine milk EVs treatment, a functional switch from very general BP to others mostly related to immune response and EVs uptake processes occurred.

### DP with greater changes in abundance in the PBMC incubated with milk EVs

To identify key DP that presented more significant changes in their raw abundances after porcine milk EVs treatment, their logFC was calculated. The protein with the highest amount after treatment with milk EVs was  $\beta$ -casein (CSN2), one of the most abundant proteins in milk. Besides nourishing the offspring by being a significant source of amino acids, caseins also have immunomodulatory effects, being broken down into immunomodulatory peptides<sup>58,59</sup>. Alpha-s1-casein (CSN1S1) and Alpha-s2-casein (CSN1S2) were also found but in lesser abundance than CSN2. After proteomics analyses, CSN2 and CSN1S1 were detected in bovine milk EVs<sup>43,60</sup>. Interestingly, CSN1S1 was shown to be expressed outside the mammary gland and to be expressed by immune cells such as monocytes and T cells<sup>61</sup>. Moreover, this protein has been shown to exert immunomodulatory effects on monocytes, such as inducing the expression of IL-1 $\beta$  and the *in vitro* differentiation towards a macrophage-like phenotype<sup>61,62</sup>.

Finally, the butyrophilin subfamily 1 member A1 (BTN1A1), Na(+)-dependent phosphate cotransporter 2B protein (SLC34A2), and MFGE8 proteins also presented greater changes in their abundance in the PBMC-treated group. BTN1A1 is a member of the immunoglobulin superfamily first discovered in milk and is mainly associated with milk fat globules. Immunomodulatory roles of this protein have also been reported, primarily inhibitory effects on CD4+ T cell proliferation and T cell expression of cytokines associated with T cell activation<sup>63</sup>[96]. The SLC34A2 is a multi-pass membrane protein that has been involved in the activation of the complement alternative pathway (C3 and C4b)<sup>64,65</sup>, while MFGE8 function has been previously described<sup>31,33,35</sup>.

On the contrary, lower abundances in the fatty acid-binding protein 4 (FABP4) and galectin-3 (LGALS3) were found. FABP4 is a protein that plays a crucial role in fatty acid transportation and functions as a transmitter linking fatty acid metabolism to inflammation. LGALS3 is a carbohydrate-binding protein highly expressed in monocytes and macrophages and a potent regulator of cell migration and phagocytosis, among other immune and inflammation-related processes<sup>66,67</sup>.

In conclusion, the results of this study demonstrate for the first time that porcine milk EVs can modulate porcine PBMC proteome *in vitro*. The GO enrichment analysis revealed that the DP with higher abundance in

the porcine milk EVs group mainly were related to innate immune-related processes. Our results also suggest that porcine milk EVs might exert pleiotropic immunomodulatory functions on PBMC by increasing the abundance of proteins with both immune-enhancing and dampening properties. Therefore, these results confirm the suppressive and enhancing effects of porcine milk EVs on porcine monocytes, observed in our previous *in vitro* study, where a decrease in the cells' phagocytosis and chemotaxis and an increase in their oxidative burst was detected. Moreover, detecting caseins and other milk proteins with known immunomodulatory properties exemplifies how EVs could fulfill their functions in intercellular communication by transferring their cargo to target cells. By providing a molecular background of porcine milk EVs' immunomodulatory activity, we can better understand their potential role in the sow-to-piglet transmission of regulatory molecules and immunomodulation. The main limitation of the present study is that it provides only a partial explanation of the molecular background of the EV immunomodulatory activity, focused on the protein content. The EV cargo contains several other molecules, like microRNA and very specific lipid specie asset. Future studies should aim to characterize these molecules as well, and their interaction with the proteome. Finally, additional molecular pathway enrichment, protein–protein interaction analyses, and integration of proteomics data with other OMIC technologies should be performed to have a holistic view of the impact of porcine milk EVs on porcine immunity.

## Materials and methods

### Experimental design

The present study aims to determine the proteome of porcine peripheral blood mononuclear cells (PBMC) after co-incubation with purified EVs from sow milk.

Porcine PBMC were isolated from blood and co-incubated with porcine EVs purified from milk. The experiment was carried out in triplicate. Proteins were extracted from cells, and the proteome was determined by Nano-LC-MS/MS analysis.

### Purification of porcine PBMC from blood

Porcine PBMC were isolated from peripheral blood through Ficoll density gradient centrifugation, as previously described for bovine blood, with some minor modifications<sup>68</sup>. Briefly, 100 mL of blood from seven 60–100 kg healthy pigs (Topigs Norsvin Italia S.r.l., Italy) was collected during routine slaughtering procedures in sterile flasks containing 0.2% of EDTA (Sigma-Aldrich, St. Louis, MO, USA) as an anticoagulant. Blood was then centrifuged at 1260×g for 30 min at 18 °C to obtain the buffy coat. The buffy coat was diluted 1:5 in cold sterile Dulbecco's PBS without Ca<sup>2+</sup> and Mg<sup>2+</sup> + 2 mM EDTA (Sigma-Aldrich), carefully layered onto Ficoll-Paque Plus (1.077 g/mL) (GE Healthcare Bio-Sciences AB, Uppsala, Sweden), and centrifuged at 1700×g (without brakes) for 30 min at 4 °C to obtain the PBMC ring. PBMC were collected at the interface, washed with cold, sterile PBS without Ca<sup>2+</sup> and Mg<sup>2+</sup> + 2 mM EDTA, centrifuged at 500×g for 7 min at 4 °C and incubated with Red Blood Cell Lysis buffer (Roche Diagnostics GmbH, Mannheim, Germany) for 3 min at room temperature to remove the red blood cells. Washes with cold sterile PBS + 2 mM EDTA were performed to remove contaminant platelets. Finally, the PBMC were counted using an automatic cell counter (TC20TM, BioRad). Their viability was assessed with trypan blue exclusion and resuspended at the desired concentration in complete medium (RPMI 1640 Medium + 25 mM HEPES + L-Glutamine, supplemented with 1% of Non-essential Amino Acid Solution 100X and 1% Penicillin Streptomycin Solution 100X and 1% EVs -depleted Fetal Bovine Serum (FBS) (Sigma-Aldrich).

### PBMC stimulation with porcine milk EVs

First, porcine milk EVs were purified from sows' milk and characterized using their concentration, size, morphology/structure, and presence of EVs marker protein, as previously reported<sup>14</sup>. An aliquot of LPS-depleted porcine milk EVs (6.2×10<sup>10</sup> EVs /mL) was thawed and used for each experiment. Briefly, a total of 15×10<sup>6</sup> porcine PBMC (1.5 mL) were seeded in triplicates in Corning® tissue-culture treated culture 60 mm dishes (Corning Inc., Costar, Kennebunk, ME, USA) and incubated with 3×10<sup>9</sup> porcine milk EVs (in a ratio of 200 EV/cell) for 22 h at 39 °C in a humidified atmosphere with 5% CO<sub>2</sub>. A complete medium (1% EVs -depleted FBS) was added to each dish to reach a final volume of 3 mL.

The utilized ratio of EVs /cell was selected based on the immunomodulatory effects previously observed *in vitro* using a similar range of 10<sup>6</sup>–10<sup>8</sup> EVs on rhesus macaques' PBMC and T cells<sup>69</sup> and in our previous study on porcine monocytes, where we did not observe toxic effects on porcine monocytes<sup>14</sup>. Seven biological replicates (animals) were used for the experiment, and the cells from each animal were seeded and treated in three technical replicates. All the following steps, including the porcine PBMC collection and protein extraction and the following proteomics procedures were carried out as previously described, with minor changes<sup>70</sup>.

### Porcine PBMC collection and protein extraction

After incubation, 3 mL of the cells in suspension (lymphocytes) were collected and centrifuged at 500×g for 7 min at 4 °C. The lymphocytes were washed twice with 500 µL sterile-PBS without Ca<sup>2+</sup> and Mg<sup>2+</sup> (room temperature) and centrifuged twice at 500×g for 7 min at 4 °C to remove the remaining medium and FBS. In the meantime, three washes with 2 mL of sterile-PBS without Ca<sup>2+</sup> and Mg<sup>2+</sup> (room temperature) were performed in the 60 mm dishes to wash the adhered monocytes and remove dead cells. When both the lymphocytes pellet and the adhered monocytes were washed, 500 µL of Igepal buffer (150 mM NaCl, 10 mM Tris-HCl pH 7.4, 1 mM EDTA and EGTA, 100 mM NaF, 4 mM Na<sub>4</sub>P<sub>2</sub>O<sub>7</sub>·10 H<sub>2</sub>O, 2 mM Na<sub>3</sub>VO<sub>4</sub>, 1% Triton X100, 0.5% IGEPAL CA-630 (Sigma-Aldrich), 1 pill for 50 mL of the total volume of Protease Inhibitor Cocktail (Roche) was added to the lymphocytes pellet. The lymphocytes were resuspended and added directly to the 60 mm dishes containing the monocytes. The plates containing the cells and the Igepal buffer were incubated for 1 h at 4 °C with regular shaking to allow the lysis of the cells. After incubation, the cells were scraped using sterile Corning Cell scrapers

(blade L 1.8 cm, handle L 25 cm; Corning Inc.), and the cell lysate was collected and sonicated for 10 min in an ultrasonic bath (Branson 2200, Danbury, CT, USA) to complete the cells' lysis and homogenization. Finally, the cell lysates were centrifuged for 10 min at  $6000 \times g$  at  $4^\circ\text{C}$  to remove the cell debris, and the supernatant containing the extracted proteins of all 3 technical replicates for each biological replicate was pooled in 1.5 mL tubes, aliquoted and stored at  $-80^\circ\text{C}$  for further analyses.

### Sample preparation for proteomic analysis

The sample preparation for proteomic was carried out as previously described, with minor changes<sup>70</sup>. The total protein concentration was determined with the Pierce Bicinchoninic acid (BCA) protein assay kit (Thermo Fisher Scientific, Rockford, IL, USA), following the manufacturer's instructions. For peptide preparation, extracted proteins were digested and concentrated using the Filter Aided Sample Preparation (FASP) method, following the manufacturer's instructions with minor modifications. Briefly, 50  $\mu\text{g}$  of protein lysate was loaded into Millipore 10 kDa MWCO filters, and 100  $\mu\text{L}$  of Urea 8 M in 0.1 M Tris-HCl pH 8.5 were added for solubilization. The detergent and other contaminant components within the protein lysate were removed by repeated filtration by centrifugation. After discarding the flow-through, proteins were reduced with 100  $\mu\text{L}$  DTT (10 mM) for 46 min and centrifuged at  $16,100 \times g$  for 10 min. Then, 200  $\mu\text{L}$  of 25 mM iodoacetamide solution were added to the filters and incubated for 20 min at room temperature for protein alkylation. After performing several washes of the filters with Urea 8 M and 50 mM of ammonium bicarbonate, proteins were digested with 200  $\mu\text{L}$  of 0.25 mg/mL trypsin (50:1 ratio of protein:enzyme) and mixed under gentle agitation in a thermomixer for 1 min. Filters were transferred to new collection tubes and incubated overnight in a wet chamber at  $37^\circ\text{C}$ . Finally, peptides were eluted by adding 200  $\mu\text{L}$  of 50 mM of ammonium bicarbonate, and the filtrate was concentrated in a SpeedVac and then resuspended in 30  $\mu\text{L}$  of 1% formic acid. The final volume was adjusted to 300  $\mu\text{L}$  with a recovery solution ( $\text{H}_2\text{O}/\text{ACN}/\text{TFA} = 94.95/5/0.05$ ). After passing through the ultrasonic bath (10 min), the supernatant was transferred to an HPLC vial before LC-MS/MS analysis.

### Nano-LC-MS/MS analysis

Peptide mixtures were analyzed by nano-LC-MS/MS (ThermoFisher Scientific) using an Ultimate 3000 system coupled to a QExactive HF-X mass spectrometer (MS) with a nanoelectrospray ion source. Five  $\mu\text{L}$  of hydrolysate was first pre-concentrated and desalted at a flow rate of 30  $\mu\text{L}/\text{min}$  on a C18 pre-column 5 cm length  $\times$  100  $\mu\text{m}$  (Acclaim PepMap 100 C18, 5  $\mu\text{m}$ , 100A nanoViper) equilibrated with Trifluoroacetic Acid 0.05% in water. After 6 min, the concentration column was switched online with a nanobebit analytical C18 column (Acclaim PepMap 100–75  $\mu\text{m}$  inner diameter  $\times$  25 cm length; C18–3  $\mu\text{m}$ –100 Å–SN 20,106,770) operating at 400 nL/min equilibrated with 96% solvent A (99.9%  $\text{H}_2\text{O}$ , 0.1% formic acid). The peptides were then separated according to their hydrophobicity thanks to a gradient of solvent B (99.9% acetonitrile, 0.1% formic acid) of 4–25% in 60 min. For MS analysis, eluted peptides were electrosprayed in positive-ion mode at 1.6 kV through a Nano electrospray ion source heated to  $250^\circ\text{C}$ . The mass spectrometer operated in data-dependent mode: the parent ion is selected in the orbitrap cell (FTMS) at a resolution of 60,000, and 18 MS/MS succeeds each MS analysis with analysis of the MS/MS fragments at a resolution of 15,000).

### Processing of raw mass spectrometry data

At the end of the LC-MS/MS analysis, for raw data processing, an MS/MS ion search was carried out with Mascot v2.5.1 (<http://www.matrixscience.com>) against the porcine database (i.e., ref\_sus\_scrofa 20,210,114–49,792 sequences). The following parameters were used during the request: precursor mass tolerance of 10 ppm and fragment mass tolerance of 0.02 Da, a maximum of two missed cleavage sites of trypsin, carbamidomethylation (C), oxidation (M) and deamidation (NQ) set as variable modifications. Protein identification was validated with a False Discovery Rate of 1% with at least two peptides originating from one protein showing statistically significant identity above Mascot score  $> 32$  and a Mascot Significance Threshold adjusted  $p$ -value 0.02747. Ions score is  $-10 \log(P)$ , where  $P$  is the probability that an observed match is a random event. Finally, LC-Progenesis QI software (version 4.2, Nonlinear Dynamics, Newcastle upon Tyne, UK) was used for label-free protein quantification analysis with the same identification parameters described above with the phenotypic data among all matrices. All unique validated peptides of an identified protein were included, and the total cumulative abundance was calculated by summing the abundances of all peptides allocated to the respective protein. LC-Progenesis analysis yielded 1584 unique quantifiable proteins, with at least two unique peptides.

### Statistical analyses

To identify the differentially abundant proteins, a univariate statistical approach was performed on all 1584 quantified proteins, using an R package for proteomic analysis (available on GitHub with the DOI <https://doi.org/10.5281/zenodo.2539329>) as previously described<sup>71</sup>. Briefly, data normality distribution was assessed by the Shapiro–Wilk-Test. Then, either a paired Student's  $t$ -test for normally distributed data or a paired Wilcoxon test for not normally distributed data was applied to determine the  $p$ -value. Finally, the obtained  $p$ -values were corrected using different adjustment methods (e.g., Benjamini & Hochberg or FDR, Hochberg, and Bonferroni). For all of these analyses, R version 4.2.2 was used.

An alternative supervised multilevel sparse variant partial least square discriminant analysis (sPLS-DA) was applied as no differentially abundant proteins were detected using the  $t$ -test or Wilcoxon tests. The multilevel sPLS-DA enables the selection of the most predictive or discriminant proteins in the data of the two components (PC1 and PC2) to classify or cluster the samples between the treatment groups<sup>20</sup>. The multivariate analysis used the mixOmics package in R (<http://mixomics.org>).



## Bioinformatic analysis of discriminant proteins (DP) selected by sPLS-DA

First, before performing the bioinformatic and functional annotation analyses, the accession numbers from all 1584 quantified proteins were converted into Gene ID using the UniProt retrieve/ID mapping online tool. The Gene ID of human orthologs of porcine proteins was assigned for undefined proteins. Second, only for the selected DP a gene ontology (GO) enrichment analysis focused on the Biological Processes (BP) was performed using ProteINSIDE online tool version 2.0 (available at [https://umrh-bioinfo.clermont.inrae.fr/ProteINSIDE\\_2/index.php?page=upload.php](https://umrh-bioinfo.clermont.inrae.fr/ProteINSIDE_2/index.php?page=upload.php)), as previously described, and using *Sus scrofa* as reference specie. Only significant (FDR < 0.05) GO BP terms were considered enriched and were used for further interpretation and figure creation. The enriched GO BP, CC, MF and KEGG<sup>72</sup> terms were summarized, and their enrichments were expressed as  $-\log_{10}$  (FDR) for visualization on horizontal bar graphs plotted using GraphPad Prism 9.1.2 for Mac OS X, GraphPad Software (San Diego, California, USA) and the ProteINSIDE online tool. Finally, the average log fold-change (logFC) of the raw abundances of all the DP identified with sPLS-DA from all seven 7 biological replicates was calculated and plotted using R version 4.2.2. Selected DP were also subjected to Protein–Protein interaction (PPI) analyses using the ProteINSIDE online tool version 2.0 to identify the proteins that have been experimentally detected to interact with each other. For the PPI analyses *Homo sapiens* was used as reference specie due to the limited number of known PPI in pigs. The PPI databases used were BAR; DIP; EBI-GOA-nonIntAct; HPIDb; IMEx; IntAct; MBInfo; MINT; MPIDB; MatrixDB; Reactome; UniProt; VirHostNet; bhf-uc; mentha and tfact2gene. The network obtained for the 54 DP related to the EVs group was reduced by filtering using betweenness centrality values algorithm of 0 to 1, which is efficient in selecting key nodes/proteins within a pathway. For the network obtained for 142 DP related to the control group betweenness centrality values of 500 to 2537 were used.

## Data availability

All data generated or analyzed during this study are included in this published article [and its supplementary information files].

Received: 21 August 2024; Accepted: 28 February 2025

Published online: 08 March 2025

## References

- Kalluri, R. & LeBleu, V. S. The biology, function, and biomedical applications of exosomes. *Science* **367**(6478), eaau6977 (2020).
- Becker, A. et al. Extracellular vesicles in cancer: Cell-to-cell mediators of metastasis. *Cancer Cell* **30**, 836–848 (2016).
- Wen, C. et al. Biological roles and potential applications of immune cell-derived extracellular vesicles. *J. Extracell. Vesicles* **6**, 1–19 (2017).
- Raposo, G. & Stoorvogel, W. Extracellular vesicles: Exosomes, microvesicles, and friends. *J. Cell Biol.* **200**, 373–383 (2013).
- Chow, A. et al. Macrophage immunomodulation by breast cancer-derived exosomes requires Toll-like receptor 2-mediated activation of NF- $\kappa$ B. *Sci. Rep.* <https://doi.org/10.1038/srep05750> (2014).
- Raposo, G. et al. B lymphocytes secrete antigen-presenting vesicles. *J. Exp. Med.* **183**, 1161–1172 (1996).
- Chaput, N. & Théry, C. Exosomes: Immune properties and potential clinical implementations. *Semin. Immunopathol.* **33**, 419–440 (2011).
- Dalvi, P., Sun, B., Tang, N. & Pulliam, L. Immune activated monocyte exosomes alter microRNAs in brain endothelial cells and initiate an inflammatory response through the TLR4/MyD88 pathway. *Sci. Rep.* **7**, 1–12 (2017).
- Chen, W. et al. Immunomodulatory effects of mesenchymal stromal cells-derived exosome. *Immunol. Res.* **64**, 831–840 (2016).
- Admyre, C. et al. Exosomes with immune modulatory features are present in human breast milk. *J. Immunol.* **179**, 1969–1978 (2007).
- Lässer, C. et al. Human saliva, plasma and breast milk exosomes contain RNA: Uptake by macrophages. *J. Transl. Med.* **9**, 9 (2011).
- Izumi, H. et al. Bovine milk exosomes contain microRNA and mRNA and are taken up by human macrophages. *J. Dairy Sci.* **98**, 2920–2933 (2015).
- Manca, S. et al. Milk exosomes are bioavailable and distinct microRNA cargos have unique tissue distribution patterns. *Sci. Rep.* **8**, 11321 (2018).
- Ávila Morales, G. et al. Porcine milk exosomes modulate the immune functions of CD14<sup>+</sup> monocytes in vitro. *Sci. Rep.* **13**, 21447 (2023).
- Pardanani, A., Wieben, E. D., Spelsberg, T. C. & Tefferi, A. Primer on medical genomics part IV: Expression proteomics. *Mayo Clin. Proceed.* **77**, 1185–1196 (2002).
- Sun, J., Shi, Z., Guo, H. & Tu, C. Changes in the porcine peripheral blood mononuclear cell proteome induced by infection with highly virulent classical swine fever virus. *J. Gen. Virol.* **91**, 2254–2262 (2010).
- Valent, D. et al. Effects on pig immunophysiology, PBMC proteome and brain neurotransmitters caused by group mixing stress and human-animal relationship. *PLoS One* **12**, 0176928–0176928 (2017).
- Chae, J.-I. et al. Quantitative proteomic analysis of pregnancy-related proteins from peripheral blood mononuclear cells during pregnancy in pigs. *Anim. Reprod. Sci.* **134**, 164–176 (2012).
- Ramirez-Boo, M. et al. Analysis of porcine peripheral blood mononuclear cells proteome by 2-DE and MS: Analytical and biological variability in the protein expression level and protein identification. *Proteomics* **6**, 215–225 (2006).
- Lê Cao, K.-A., Boitard, S. & Besse, P. Sparse PLS discriminant analysis: Biologically relevant feature selection and graphical displays for multiclass problems. *BMC Bioinform.* **12**, 253 (2011).
- May, R. C. & Machesky, L. M. Phagocytosis and the actin cytoskeleton. *J. Cell Sci.* **114**, 1061–1077 (2001).
- Affolter, M. & Weijer, C. J. Signaling to cytoskeletal dynamics during chemotaxis. *Dev. Cell* **9**, 19–34 (2005).
- Roy, N. H. & Burkhardt, J. K. The actin cytoskeleton: A mechanical intermediate for signal integration at the immunological synapse. *Front. Cell Dev. Biol.* <https://doi.org/10.3389/fcell.2018.00116> (2018).
- Brown, E., Weering, J., Sharp, T., Mantell, J. & Verkade, P. Chapter 10 - Capturing endocytic segregation events with HPF-CLEM. In *Light Electron Microscopy* (Academic Press, 2012). <https://doi.org/10.1016/B978-0-12-416026-2.00010-8>.
- Knaap, J. A. & Verrijzer, C. P. Undercover: Gene control by metabolites and metabolic enzymes. *Genes Dev.* **30**, 2345–2369 (2016).
- Uribe-Querol, E. & Rosales, C. Phagocytosis our current understanding of a universal biological process. *Front. Immunol.* <https://doi.org/10.3389/fimmu.2020.010663> (2020).
- Kalluri, R. The biology and function of exosomes in cancer. *J. Clin. Invest.* **126**, 1208–1215 (2016).

28. Silverstein, R. L. & Febbraio, M. CD36 a scavenger receptor involved in immunity metabolism, angiogenesis and behavior. *Sci. Signal* **2**, 3–3 (2009).
29. Baranova, I. N. et al. Role of human CD36 in bacterial recognition phagocytosis and pathogen-induced JNK-mediated signaling. *J. Immunol* **181**, 7147–71563 (2008).
30. Park, Y. M., Febbraio, M. & Silverstein, R. L. CD36 modulates migration of mouse and human macrophages in response to oxidized LDL and may contribute to macrophage trapping in the arterial intima. *J. Clin. Invest* **119**, 136–145 (2009).
31. Sugano, G. et al. Milk fat globule—epidermal growth factor—factor VIII (MFG8)/lactadherin promotes bladder tumor development. *Oncogene* **30**, 642–653 (2010).
32. Dasgupta, S. K. & Thiagarajan, P. The role of lactadherin in the phagocytosis of phosphatidylserine-expressing sickle red blood cell by macrophages. *Blood* **106**, 3773 (2005).
33. Zhou, Y.-J. et al. The role of the lactadherin in promoting intestinal DCs development in vivo and vitro. *Clin. Dev. Immunol.* <https://doi.org/10.1155/2010/357541> (2010).
34. Magdanz, V., Boryshpolets, S., Ridzewski, C., Eckel, B. & Reinhardt, K. The motility-based swim-up technique separates bull sperm based on differences in metabolic rates and tail length. *PLoS One* **42**, 400 (2019).
35. Reinhardt, T. A., Lippolis, J. D., Nonnecke, B. J. & Sacco, R. E. Bovine milk exosome proteome. *J. Proteomics* **75**, 1486–1492 (2012).
36. Murphy, D. E. et al. Extracellular vesicle-based therapeutics: Natural versus engineered targeting and trafficking. *Exp. Mol. Med* **51**, 1–12 (2019).
37. Wortzel, I. & Seger, R. The ERK cascade: Distinct functions within various subcellular organelles. *Genes Cancer* **2**, 195–209 (2011).
38. Svensson, K. J. et al. Exosome uptake depends on ERK1/2-heat shock protein 27 signaling and lipid Raft-mediated endocytosis negatively regulated by caveolin-1. *J. Biol. Chem* **288**, 17713–17724 (2013).
39. Ma, J. et al. Mesenchymal stem cell-derived exosomal miR-21a-5p promotes M2 macrophage polarization and reduces macrophage infiltration to attenuate atherosclerosis. *Acta Biochim. Biophys. Sin.* **53**, 1227–1236 (2021).
40. Getz, G. S. & Reardon, C. A. Apoproteins E, A-I, and SAA in macrophage pathobiology related to atherogenesis. *Front. Pharmacol* <https://doi.org/10.3389/fphar.2019.00536> (2019).
41. Baitsch, D. et al. Apolipoprotein E induces anti-inflammatory phenotype macrophages. *Arter. Thromb. Vasc. Biol* **31**, 1160–1168 (2011).
42. Zheng, P. et al. Tumor-associated macrophages-derived exosomes promote the migration of gastric cancer cells by transfer of functional apolipoprotein E. *Cell Death Dis* **9**, 434 (2018).
43. Ferreira, R. F. et al. Comparative proteome profiling in exosomes derived from porcine colostrum versus mature milk reveals distinct functional proteomes. *J. Proteomics* <https://doi.org/10.1016/j.jprot.2021.104338> (2021).
44. Wang, H., Du, S., Cai, J., Wang, J. & Shen, X. Apolipoprotein E2 promotes the migration and invasion of pancreatic cancer cells via activation of the ERK1/2 signaling pathway. *Cancer Manag. Res* **12**, 13161–13171 (2020).
45. Lee, J. Y., Park, J. K., Lee, E. Y., Lee, E. B. & Song, Y. W. Circulating exosomes from patients with systemic lupus erythematosus induce a proinflammatory immune response. *Arthritis. Res. Ther.* **18**, 264 (2016).
46. Abdul-Cader, M. S., Amarasinghe, A. & Abdul-Careem, M. F. Activation of toll-like receptor signaling pathways leading to nitric oxide-mediated antiviral responses. *Arch. Virol.* **161**, 2075–2086 (2016).
47. Li, H. et al. Coronary serum exosomes derived from patients with myocardial ischemia regulate angiogenesis through the miR-939-mediated nitric oxide signaling pathway. *Theranostics* <https://doi.org/10.7150/thno.21895> (2018).
48. Hattori, H. et al. Senescent RAW2647 cells exhibit increased production of nitric oxide and release inducible nitric oxide synthase in exosomes. *Mol. Med. Rep.* **24**, 681 (2021).
49. Tan, X.-H. et al. Skimmed bovine milk-derived extracellular vesicles isolated via 'Salting-Out': Characterizations and potential functions as nanocarriers. *Front Nutr* <https://doi.org/10.3389/fnut.2021.769223> (2021).
50. Weng, X. et al. Clusterin regulates macrophage expansion, polarization and phagocytic activity in response to inflammation in the kidneys. *Immunol. Cell Biol.* **99**, 274–287 (2020).
51. Cunin, P. et al. Clusterin facilitates apoptotic cell clearance and prevents apoptotic cell-induced autoimmune responses. *Cell Death Dis.* **7**, 2215–2215 (2016).
52. Cintio, M. et al. MicroRNA milk exosomes: From cellular regulator to genomic marker. *Animal* <https://doi.org/10.3390/ani10071126> (2020).
53. Delmonte, O. M. et al. SASH3 variants cause a novel form of X-linked combined immunodeficiency with immune dysregulation. *Blood* **138**, 1019–1033 (2021).
54. Wang, X. et al. Proteomic analysis and cross species comparison of casein fractions from the milk of dairy animals. *Sci. Rep.* <https://doi.org/10.1038/srep43020> (2017).
55. Aminzadeh, M. A. et al. Casein-enhanced uptake and disease-modifying bioactivity of ingested extracellular vesicles. *J. Extracell. Vesicles* **10**, 12045 (2021).
56. Malagobadan, S. & Nagoor, N. H. *Anoikis* (Academic Press, 2017). <https://doi.org/10.1016/B978-0-12-801238-3.65021-3>.
57. Aparicio-Siegmund, S. & Garbers, C. The biology of interleukin-27 reveals unique pro- and anti-inflammatory functions in immunity. *Cytokine Growth Factor Rev.* **26**, 579–586 (2015).
58. Wheeler, T. T., Hodgkinson, A. J., Prosser, C. G. & Davis, S. R. Immune components of colostrum and milk—A historical perspective. *J. Mammary Gland Biol., Neoplasia* **12**, 237–247 (2007).
59. Sadler, M. J. & Smith, N. Beta-casein proteins and infant growth and development. *Infant J.* **9**, 173–176 (2013).
60. Samuel, M. et al. Bovine milk-derived exosomes from colostrum are enriched with proteins implicated in immune response and growth. *Sci. Rep.* **7**, 5933 (2017).
61. Vordenbäumen, S. et al. Casein  $\alpha$  s1 is expressed by human monocytes and upregulates the production of GM-CSF via p38 MAPK. *J. Immunol.* **186**, 592–601 (2011).
62. Vordenbäumen, S. et al. Human casein  $\alpha$  s1 (CSN1S1) skews in vitro differentiation of monocytes towards macrophages. *BMC Immunol.* **14**, 46 (2013).
63. Arnett, H. A. & Viney, J. L. Immune modulation by butyrophilins. *Nat. Rev. Immunol* **14**, 559–569 (2014).
64. Wang, Y. et al. The effects and mechanisms of SLC34A2 in tumorigenesis and progression of human non-small cell lung cancer. *J. Biomed. Sci.* **22**, 52 (2015).
65. Yang, W. et al. Elevated expression of SLC34A2 inhibits the viability and invasion of A549 cells. *Mol. Med. Rep* **10**, 1205–1214 (2014).
66. Brinckmann, M. F., Patel, D. M. & Iversen, M. H. The role of galectins as modulators of metabolism and inflammation. *Mediat. Inflamm.* **2018**, 9186940 (2018).
67. Lu, Y. et al. Modified citrus pectin inhibits galectin-3 function to reduce atherosclerotic lesions in apoE-deficient mice. *Mol. Med. Rep.* **16**, 647–653 (2017).
68. Cecilian, F. et al. Methods in isolation and characterization of bovine monocytes and macrophages. *Methods* <https://doi.org/10.1016/j.ymeth.2020.06.017> (2020).
69. Hong, X., Schouest, B. & Xu, H. Effects of exosome on the activation of CD4+ T cells in rhesus macaques: A potential application for HIV latency reactivation. *Sci. Rep.* **7**, 15611 (2017).
70. Ávila, G. et al. Conjugated linoleic acid (CLA) modulates bovine peripheral blood mononuclear cells (PBMC) proteome in vitro. *J. Proteomics* **304**, 105232 (2024).

71. Bazile, J., Picard, B., Chambon, C., Valais, A. & Bonnet, M. Pathways and biomarkers of marbling and carcass fat deposition in bovine revealed by a combination of gel-based and gel-free proteomic analyses. *Meat Sci.* **156**, 146–155 (2019).
72. Kanehisa, M., Furumichi, M., Sato, Y., Matsuura, Y. & Ishiguro-Watanabe, M. KEGG: Biological systems database as a model of the real world. *Nucl. Acids Res.* **53**, D672–D677 (2025).

## Acknowledgements

The authors acknowledge A. Delavaud (INRAE, Herbivore Research Unit) for his technical assistance in protein extraction, quantification, and concentration for mass spectrometry analyses, and also Arnaud Cougoul, Jeremy Tournayre and Céline Boby (INRAE, Herbivore Research Unit) for their assistance in the statistical and bioinformatic analyses, respectively. The authors acknowledge support from the Università degli Studi di Milano through the APC initiative.

## Author contributions

G. Ávila: Writing—original draft, Software, Methodology, Investigation, Formal analysis, Conceptualization. F. Cecilian: Writing—review & editing, Writing—original draft, Validation, Supervision, Project administration, Funding acquisition, Conceptualization. D. Viala: Writing—original draft, Software, Resources, Methodology, Formal analysis, Data curation. S. Dejean: Writing—review & editing, Software, Resources, Formal analysis, Data curation. A. Agazzi: Resources, Methodology. C. Lecchi: Writing—review & editing, Validation. M. Bonnet: Writing—review & editing.

## Funding

This study was supported by the European Union's Horizon 2020 research and innovation program H2020-MS-CA- ITN-2017- EJD: Marie Skłodowska-Curie Innovative Training Networks (European Joint Doctorate) [Grant agreement n°: 765423, 2017] – MANNA.

## Declarations

### Competing interests

The authors declare no competing interests.

### Ethical approval

The procedures for the blood collection were carried out during routine slaughtering procedures. The milk collection from sows was carried out in the frame of a study approved by the Ethical Committee of the University of Milan (OPBA 67/2018) and the Italian Ministry of Health (authorization n. 168/2019 PR).

### Consent for publication

Not applicable.

### Additional information

**Supplementary Information** The online version contains supplementary material available at <https://doi.org/10.1038/s41598-025-92550-3>.

**Correspondence** and requests for materials should be addressed to F.C.

**Reprints and permissions information** is available at [www.nature.com/reprints](http://www.nature.com/reprints).

**Publisher's note** Springer Nature remains neutral with regard to jurisdictional claims in published maps and institutional affiliations.

**Open Access** This article is licensed under a Creative Commons Attribution-NonCommercial-NoDerivatives 4.0 International License, which permits any non-commercial use, sharing, distribution and reproduction in any medium or format, as long as you give appropriate credit to the original author(s) and the source, provide a link to the Creative Commons licence, and indicate if you modified the licensed material. You do not have permission under this licence to share adapted material derived from this article or parts of it. The images or other third party material in this article are included in the article's Creative Commons licence, unless indicated otherwise in a credit line to the material. If material is not included in the article's Creative Commons licence and your intended use is not permitted by statutory regulation or exceeds the permitted use, you will need to obtain permission directly from the copyright holder. To view a copy of this licence, visit <http://creativecommons.org/licenses/by-nc-nd/4.0/>.

© The Author(s) 2025